69th International Astronautical Congress 2018, Bremen, Germany, 1-5 October 2018

END-OF-LIFE DISPOSAL DESIGN FOR SPACECRAFT AT LIBRATION POINTS ORBITS AND AN INTERPRETATION OF THEIR PROBABILITY OF EARTH RETURN

Greta De Marco[1], Camilla Colombo[2].

[1] Politecnico di Milano, Dep. of Aerospace Science and Technology, Milano, Italy; greta.demarco@mail.polimi.it
[2] Politecnico di Milano, Dep. of Aerospace Science and Technology, Milano, Italy; camilla.colombo@polimi.it

Since the beginning of space activities, the number of spacecraft completing their missions keep rising, thus increasing the amount of inoperative spacecraft and space debris which could collide with operative spacecraft or re-enter to Earth in an uncontrolled manner. No guidelines currently exist for spacecraft orbiting about Lagrangian points; as orbits about them are increasingly being selected for future missions, it is important to safely dispose spacecraft at the end of their life. This goal is sometimes achieved performing a non-optimal single disposal manoeuvre directed along the Sun-Earth line direction to reduce the operational cost during the disposal phase. This paper will instead optimise such a manoeuvre dividing it in, at least, two consecutive burns, even in the case in which the total available Δv is low. In this work we will analyse the optimal disposal manoeuvre design using the elliptical restricted three-body problem and the energetic approach firstly introduced for the circular restricted three-body problem by Olikara et al. The disposal design is performed for the Gaia and Lisa Pathfinder missions for different initial conditions over one year. Finally, an interpretation of the results of a long-term simulation of the disposal orbit in the n-body problem is given, by analysing the probability of return to Earth against the date when the disposal manoeuvre is given.

1 Introduction

Libration Point Orbits (LPOs) are increasingly selected for science mission due to the favourable conditions they ensure for thermal stability, continuous communication with Earth and low-cost station keeping. Example of spacecraft orbiting libration points, are SOHO, ISEE-3, Lisa pathfinder, Gaia, Athena and JWST. Currently no guidelines exist to dispose them [1] and, since the dynamical environment at the Lagrangian points is highly perturbed, it is important to avoid an uncontrolled return to Earth of the spacecraft after the end-of-life of the spacecraft, unless planned by the mission operations. Various possible disposal strategies for spacecraft at LPOs were studied in the past. A spacecraft in LPO can be disposed through Moon impact (Colombo et al. [2]), Earth re-entry (Alessi et al. [3], Colombo et al. [4]) or displaced in a heliocentric trajectory (Olikara et al. [1], Colombo et al. [5], Soldini et al. [6]). This paper considers this last approach since it was selected by the European Space Agency (ESA) to dispose the Hershel and Lisa pathfinder spacecraft. Olikara et al. [1] used a Circular Restricted Three-Body Problem (CR3BP), while Colombo et al. [5] an *n*-body model. From this last study, it emerged that there is a relation between the optimal disposal manoeuvre and the true anomaly of the Earth + Moon Barycentre (EMB) at the time of the spacecraft departure from its nominal orbit. In this paper, to take into account this dependence, and to be able to isolate and understand the role of this parameter in the disposal design, the considered model is the Elliptical Restricted Three-Body Problem (ER3BP). Moreover, this model is simple and elegant, it allows an analytic interpretation and it is a good approximation to the real problem as stated by Luo et al. [7] and Hyeraci et al. [8].

2 The elliptical restricted three-body problem

2.1 The reference frames

To describe the motion of spacecraft under the effect of two main attractors and taking into account the eccentricity in the orbit of one of the primaries, three reference frames are introduced: the inertial, the perifocal and the rotating frame (Soldini, [9]). The inertial reference frame is fixed in time and it is the mean ecliptic and equinox centred at the Sun - Earth barycentre. The perifocal reference frame has the Earth's orbit around the Sun as a reference plane, while its x-axis is directed toward the pericentre of its orbit. Finally, the rotating frame follows the Earth's rotation around the Sun. The velocity of rotation is not constant, since the orbit of the Earth is on an ellipse. Considering negligible the inclination of the Earth orbit over the ecliptic, as suggested in [9], the position vector of a generic body, $\mathbf{r}_r$, in the pulsating refence frame is defined as in Eq. (1) where $\mathbf{r}_i$ is its position in the inertial refence frame and $\mathbf{C}_{ri}$ is the matrix defined by Eq. (2). In this equation the terms ϑ, ω and Ω are, respectively, the Earth's true anomaly, the argument of periapsis and the right ascension of the ascending node of its orbit.

$$\mathbf{r}_r = \mathbf{C}_{ri}\mathbf{r}_i \tag{1}$$

$$\mathbf{C}_{ri} = \begin{bmatrix} \cos(\vartheta+\omega+\Omega) & \sin(\vartheta+\omega+\Omega) & 0 \\ -\sin(\vartheta+\omega+\Omega) & \cos(\vartheta+\omega+\Omega) & 0 \\ 0 & 0 & 1 \end{bmatrix} \tag{2}$$

2.2 The dynamics equations

To write the equation of motion in an easier form, in the literature, for example in [10] and [11], the position vector is used in its non-dimensional form, obtained dividing $\mathbf{r}_i$ by *r* defined in Eq. (3)

, where *e* is the Earth's orbit eccentricity.

$$r = \frac{a(1-e^2)}{1+e\cos\vartheta} \tag{3}$$

In the rotating refence frame, centred at the Solar system barycentre, the x-axis is always directed as the Sun – Earth line, while the Earth and the Sun are moving along this orbit, while they orbit around the barycentre with a periodicity of one year. This pulsation can be eliminated from the equations of motion by performing the derivative of the dimensionless state vector with respect to the true anomaly ϑ, instead of the time. In this way the position of Sun and Earth are fixed in time on this frame. The resulting equations of motion, Eq.(4), have equal shape as the ones computed for the CR3BP, [10] [9]. This is possible since the only time-dependent variable in the dimensionless position vector is the true anomaly, if we consider negligible the change over time in ω and Ω.

$$\begin{cases} x'' - 2y' = \dfrac{\partial\psi}{\partial x} \\ y'' + 2x' = \dfrac{\partial\psi}{\partial x} \\ z'' = \dfrac{\partial\psi}{\partial x} \end{cases} \tag{4}$$

The apexes indicate a derivative with respect to the true anomaly and the pseudo-potential ψ is defined as:

$$\psi = \frac{1}{1+e\cos\vartheta}\left[\frac{1}{2}(x^2+y^2-ez^2\cos\vartheta)+V\right] \tag{5}$$

$$V = \frac{\mu_2}{r_{2\text{-sc}}} + \frac{\mu_1}{r_{1\text{-sc}}} \tag{6}$$

In Eq.(6), the subscript *1* indicates the Sun and the subscript *2* indicates the Earth. Indeed, x_1 and x_2 are the non-dimensional Sun and Earth position, given respectively by $x_1 = -\mu$ and $x_2 = 1-\mu$. The term μ is equal to μ_2 which is defined as $(\mu_{moon}+\mu_{earth})/(\mu_{moon}+\mu_{earth}+\mu_{sun})$. The term μ_1 is equal to $1-\mu$ and $r_{1\text{-sc}} = \sqrt{(x-x_1)^2+y^2+z^2}$ and $r_{2\text{-sc}} = \sqrt{(x-x_2)^2+y^2+z^2}$.

Thus, the dimensionless equations of motion in ER3BP are expressed as:

$$\begin{cases} x''-2y' = \dfrac{1}{1+e\cos\vartheta}\left[x-\mu_1\dfrac{x-x_1}{r_{1\text{-sc}}^3}-\mu_2\dfrac{x-x_2}{r_{2\text{-sc}}^3}\right] \\ y''+2x' = \dfrac{1}{1+e\cos\vartheta}\left[y-\mu_1\dfrac{y}{r_{1\text{-sc}}^3}-\mu_2\dfrac{y}{r_{2\text{-sc}}^3}\right] \\ z'' = \dfrac{1}{1+e\cos\vartheta}\left[-ez\cos\vartheta-\mu_1\dfrac{z}{r_{1\text{-sc}}^3}-\mu_2\dfrac{z}{r_{2\text{-sc}}^3}\right] \end{cases} \tag{7}$$

Another advantage to use the pulsating dimensionless reference frame is the one that the

libration points, points of equilibrium for the equation of motion for which $x'' = y'' = z'' = x' = y' = 0$ still exist and have the same position as the one in CR3BP (Colasurdo et al. [12]).

2.3 The energy and the zero velocity curves

In the CR3BP, it exists a constant of motion, *J*, called the Jacobi constant [10], which is related to the energy, *E*, of the spacecraft by the relation $E = -J/2$. In the ER3BP, the energy of the spacecraft is obtained multiplying Eq. (7) by, respectively, *x'*, *y'* and *z'*. Then the sum of the resulting equations and the integration of the result over the true anomaly, from ϑ to ϑ_0, yield the energy, which is composed by two terms: the relative energy E_r and an integral term *I*, [13].

$$E = E_r + I \tag{8}$$

$$E_r = \frac{1}{2}v^2 \tag{9}$$

$$v = \sqrt{x'^2 + y'^2 + z'^2} \tag{10}$$

$$I = \int_{\vartheta_0}^{\vartheta} \frac{e\sin\vartheta}{(1+e\cos\vartheta)^2} W \tag{11}$$

$$W = x^2 + y^2 + z^2 + V \tag{12}$$

In Eq. (12) V is the potential defined in Eq. (6), ϑ_0 is the true anomaly of Earth at the departure point for the numerical integration.

To solve the integral in Eq. (11) analytically it is necessary to know how *W* depends on ϑ explicitly, as explained by Luk'yanov [13]. This dependence is implicit into the spacecraft's position vector, which is obtained numerically integrating the ER3BP equations of motion, Eq. (7). Luk'yanov in 2005, demonstrated that the total energy of the spacecraft in the ER3BP is constant if the ϑ_0 is fixed, [13]. Moreover, this assumption can be demonstrated solving the integral numerically. Consequently, the Jacobi constant *J* exists even in the ER3BP.

For the purpose of explaining the selected disposal strategy, we introduce the Zero Velocity Curves (ZVCs), which give a qualitative representation of region of space in which the spacecraft is allowed to move. In Fig. 1 the black curve represents a generic ZVC which divides the space in three regions: the exterior realm, the interior realm and the forbidden region. This last one, in grey, is the region where the velocity of the spacecraft would be a complex number, which is physically impossible, meaning that in this region the spacecraft cannot move due to energetic reasons. The importance of ZVCs in the disposal will be better explained in Section 3.2, [10].

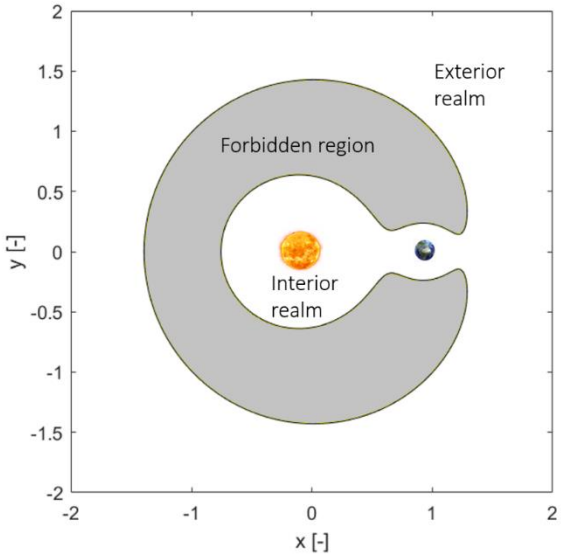

Fig. 1: Representation of the zero velocity curves.

To obtain the equation that describes the ZVCs it is sufficient to set to zero the velocity term in the Jacobi constant espression. However, in ER3BP it is not possible to have an analitical espression for them, due to the fact that the integral term cannot be analitically solved. In literature, different types of approximations were proposed [14], [15], [13]. In this paper, the one suggested by Luk'yanov in [13] with Soldini et al. modifications [6] it is used. Luk'yanov suggested to approximate the integral term in the energy as follows:

$$I = W_{min}\left(\frac{1}{1+e\cos\vartheta} - \frac{1}{1+e\cos\vartheta_0}\right) \tag{13}$$

where

$$W_{min} = \frac{1}{2}[3 + \mu(\mu - 1)] \quad (14)$$

The term W_{min} can be computed as shown in [13] and in [9], because Luk'yanov demonstrated that a minimum for the quantity *W* exists, and it is equal to Eq. (14). Thus, the zero velocity curves equation, obtained by substituting the integral term in *J* with Eq. (13) and setting the velocity *v* to zero, is represented by Eq. **Errore. L'origine riferimento non è stata trovata.**,

$$J = 2\psi - 2W_{min}\left(\frac{1}{1+e\cos\vartheta} - \frac{1}{1+e\cos\vartheta_0}\right) \quad (15)$$

Soldini et al. [6], demonstrated that this approximation is good only at Close Approaches (CA), which are defined as the region of space in the pulsating dimensionless reference frame for which $x > 0$ and $|y|<10^{-2}$, accordingly with [5]. Since we are interested only in the regions of space close to the libration points, thus in the CA region, this approximation is the ideal one.

The ZVCs are defined setting *J* equal to a constant, which is the Jacobi constant of the spacecraft, J_{sc}, as in [6]. Thus, in Eq.**Errore. L'origine riferimento non è stata trovata.**, the left-hand side should be constant and equal to J_{sc}, while the right-hand side pulsates due to the true anomaly ϑ.

3 The disposal manoeuvres strategies

As analysed by Colombo et al. in [2] and Armellin et al. in [16], the three possible options for the end-of-life for missions targeting the libration points are: disposal through semi-controlled Earth re-entry (Colombo et al. [4], Alessi et al. [3], Armellin et al. [16]), disposal through impact onto the Moon surface (Colombo et al. [17]) or the disposal toward a heliocentric orbit with the exploitation of solar radiation pressure or with an impulsive manoeuvre (Olikara et al. [1], Colombo et al. [5], Soldini et al. [6]). In this paper the latter one is presented, of which two variants are proposed: the single and the two-impulse disposal strategies.

3.1 Single impulse non-optimal disposal manoeuvre

The simple single one, given along the Sun – Earth direction, towards the Sun to enter the interior realm for missions to L_1 and in the opposite direction in the L_2 case, to enter the exterior realm of the ZVCs. This manoeuvre was the one used by ESA for Lisa pathfinder and Hershel and it is shown in Fig. 2. This solution best fits the cases in which there are some operational constraints that require to have a rapid disposal, like avoiding possible engine failure. Moreover, it might be the only choice if the available Δv is so small to not allow to give two burns. If we name respectively α and β the Δv in-plane and out-of-plane angles in the synodic reference frame, as it is shown in Fig 3 the single manoeuvre strategy corresponds to an angle $\alpha = \pi$ for missions around L_1 and $\alpha = 0$ for missions around L_2. The out-of-plane angle β is equal to zero in both cases.

Fig. 2: Single burn disposal manoeuvre representation.

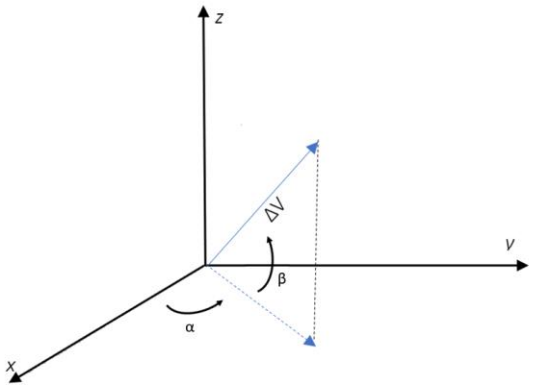

Fig. 3: Δv components in the synodic reference frame. The angle α is the in-plane angle, while the β represent the out-of-plane angle.

3.2 The energetic approach

The basic idea for the disposal is to use the energetic approach first indroduced by Olikara et al. [1] for

CR3BP, which is simply explained for Gaia in Fig. 4. This approach, also used by Colombo et al. [5], concerns in changing the spacecraft energy by applying two Δvs. Changing the spacecraft energy, means to modify the geometry of the ZVCs, indeed the manoeuvres shall be done in such a way to close them at the libration point of interest, to trap the spacecraft around L_1 in the interior realm or the spacecraft around L_2 in the exterior real. A first manoeuvre is given to let the spacecraft leave its orbit to enter the unstable manifold [18], then a second one should be given within six months, for operational reasons, to close the curves.

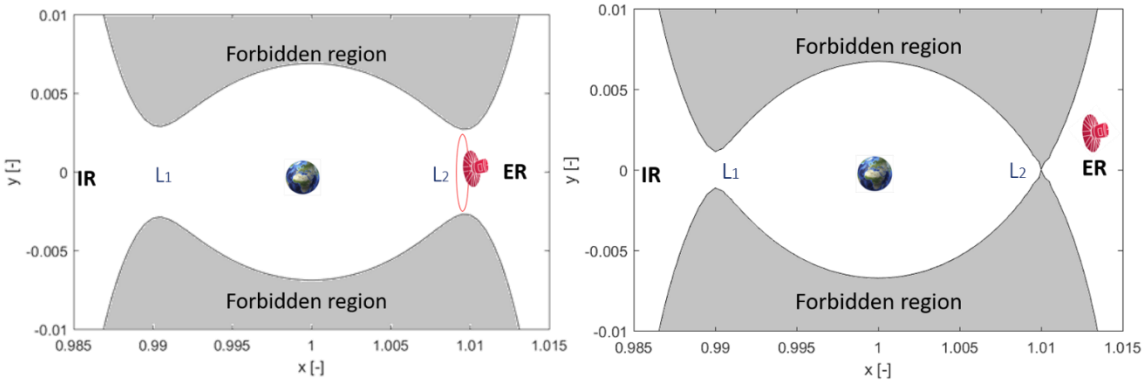

Fig. 4: Simple representation of the energetic approach for the disposal of Gaia mission. With IR is indicated the Interior Realm, while with ER the Exterior Realm. On the left, the ZVCs are opened at L_2 and Gaia Lissajous is represented with the red curve. On the right the ZVCs are closed at L_2 and Gaia is trapped in the exterior realm

In this paper, the main difference with respect to the previous work is the use of the ER3BP model in designing the optimal impulsive disposal manoeuvre, as done by Soldini et al. exploiting the effect of solar radiation pressure [6] using the propellant left on board and a new way to determine if the ZVCs are properly closed or not. Moreover, the optimal manoeuvre will be designed for both type of missions about L_1 and L_2 (Gaia and Lisa Pathfinder (LPF) has been selected as test cases).

In the ER3BP, as said in Section 3.2, the zero velocity curves pulsate with the true anomaly of the Earth ϑ, therefore it is important to clearly understand when the ZVCs are truly closed.

Before proceeding it is important to remark that, in the ER3BP:

- the energy of the spacecraft is constant for a fixed level of ϑ_0, where ϑ_0 is the true anomaly of Earth at the begging of the disposal,
- the energy evaluated at the libration points is constant and depends only on ϑ_0 (see [19]),
- the actual and the approximated ZVCs in ER3BP oscillate with a period of one solar year.

It is also important to clarify the terminology that will be used in the following lines:

- with *Jacobi constant*, we refer to the constant -2E, where *E* is the true energy of the spacecraft, defined in Eq. (8);
- with *Jacobi pseudo-constant*, we refer to the *approximated* Jacobi constant defined as:

$$J = -v^2 + 2\psi - 2W_{min}\left(\frac{1}{1+e\cos\vartheta} - \frac{1}{1+e\cos\vartheta_0}\right) \qquad (16)$$

  In the case in which the velocity *v* Eq. (16) is set to zero, the *Jacobi pseudo-constant* represents the ZVCs at CAs, indeed in this case will be named simply ZVC, Eq. (15);
- the *approximated energy* is defined as the *Jacobi pseudo-constant* multiplied by –2.

The Jacobi pseudo-constant evaluated at the libration points J_{LP}, is obtained from Eq.(16), reminding that the velocity term is equal to zero because the libration points are points of equilibrium:

$$J_{LP} = 2\psi_{LP} - 2\,W_{min}\left(\frac{1}{1+e\cos\vartheta} - \frac{1}{1+e\cos\vartheta_0}\right) \quad (17)$$

If we evaluate Eq. (17) at the libration points, the Jacobi pseudo-constant result to be equal to the ZVCs approximation for the ER3BP (called ZVC_{Li} and defined in Eq. (15), where the subscrit *i* is the number of the considered libration point) since the only difference is the velocity term, which in this case is zero due to the libration point definition. Thus, Eq. (17), gives the information about the ZVCs evolution for a body with an energy equal to the one of the libration point of interest. The ZVCs oscillates with ϑ, with a periodicity of one year, Fig. 5. More precisely, the curve gives the information about how the energy of a body should evolve to have the ZVCs just closed at the considered equilibrium point. Indeed, in the CR3BP model, it was sufficient that the Jacobi constant of the spacecraft was above the one of the libration point, to be sure that the ZVC will be closed for any following time instants. Since in the ER3BP the energies are constant, but the ZVCs have a pulsating behaviour, it is not any more sufficient to have the Jacobi constant of the spacecraft above the one evaluated at the libration point.

Thus, knowing that Eq. (15)(17) is a good approximation of the ZVCs at the CA, this value of Jacobi pseudo-constant identify the boundary between having the ZVCs opened or closed. Thus, if the spacecraft Jacobi constant, J_{SC}, is above the curve defined by Eq. (17), for a selected libration point and for a determined ϑ it means that, for that ϑ, the ZVCs are closed in correspondence of the equilibrium point.

To facilitate the understanding and to prove the validity of the method just explained, a graphical demonstration is shown in Fig. 5 and in Fig. 6. Fig. 5 shows the ZVCs evaluated at L_1 (ZVC_{L1}, in red) and at L_2 (ZVC_{L2}, in yellow), through Eq. (17). The blue line represents a generic Jacobi constant of a spacecraft. In the zoomed picture on the right, five points can be identified (x-symbols), which corresponds to different values of ϑ. The comparison between the spacecraft Jacobi constant (blue line) with the ZVCs evaluated at L_1 (red curve) and L_2 (yellow curve) for each different ϑ gives the information about the state of the ZVCs at those equilibrium points.

For the ϑ corresponding to the point A in Fig. 5, J_{SC}, is less than both ZVC_{L1} and ZVC_{L2}. Consequently, it is expected that both the bottlenecks at L_1 and at L_2 are opened. This is confirmed by Fig. 6a. The point B is located at a value of ϑ for which J_{SC} intersects ZVC_{L2}, while ZVC_{L1} does not. Thus, the bottleneck at L_2 should be just closed while the one at L_1 should be still opened because $J_{SC} < ZVC_{L1}$ for that value of ϑ. As before, Fig. 6b confirms this hypothesis. In the case of the point C, the condition is the same than point B, with the only difference that the bottleneck at L_1 is more closed with respect to the previous case (Fig. 6c). Point D has a ϑ at which J_{SC} intersects ZVC_{L1}, while $J_{SC} > ZVC_{L2}$. This means that the bottleneck at L_1 is closed at a single point (Fig. 6d), while the one at L_2 is still closed. In the last case, point E, both bottlenecks are well closed since $J_{SC} > ZVC_{L1}$ and $J_{SC} > ZVC_{L2}$ (Fig. 6e).

In conclusion, it is important to underline two facts. The first one is that the energy of the spacecraft is constant and that the ZVCs changes only because the true anomaly does, thus this method uses the evaluation of approximated ZVCs at the libration points to understand their behaviour with respect to the Jacobi constant of the spacecraft. The second fact is that the method is valid for each value of true anomaly, but, since it has been demonstrated that Eq. (17) are the exact representation of ZVCs is only valid at CAs, it can be considered valid only in this case. The CA is indeed the situation at which we want to make sure that the

c)

spacecraft does not trespass the ZVCs and re-enter in an uncontrolled way to the Earth.

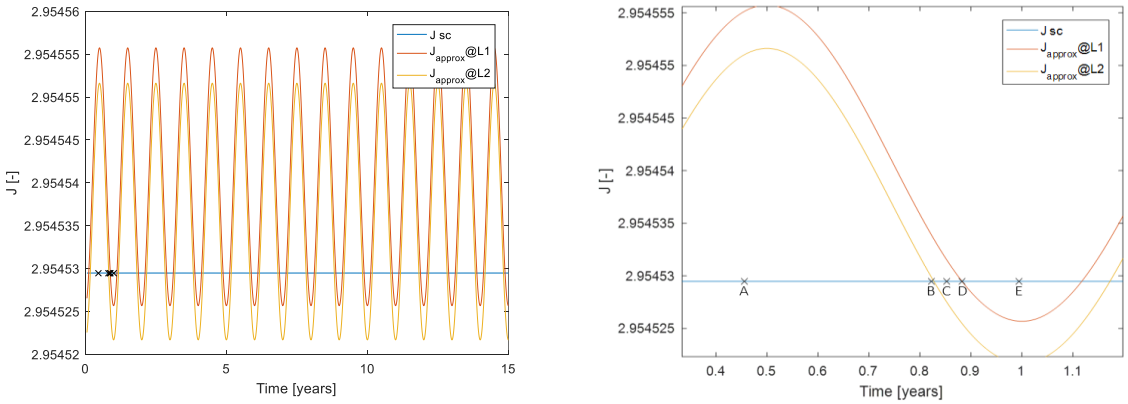

Fig. 5: Approximated ZVC evaluated at L_1 (in red) and at L_2 for $\vartheta_0 = 20°$. The blue line indicates a Jacobi constant of the spacecraft.

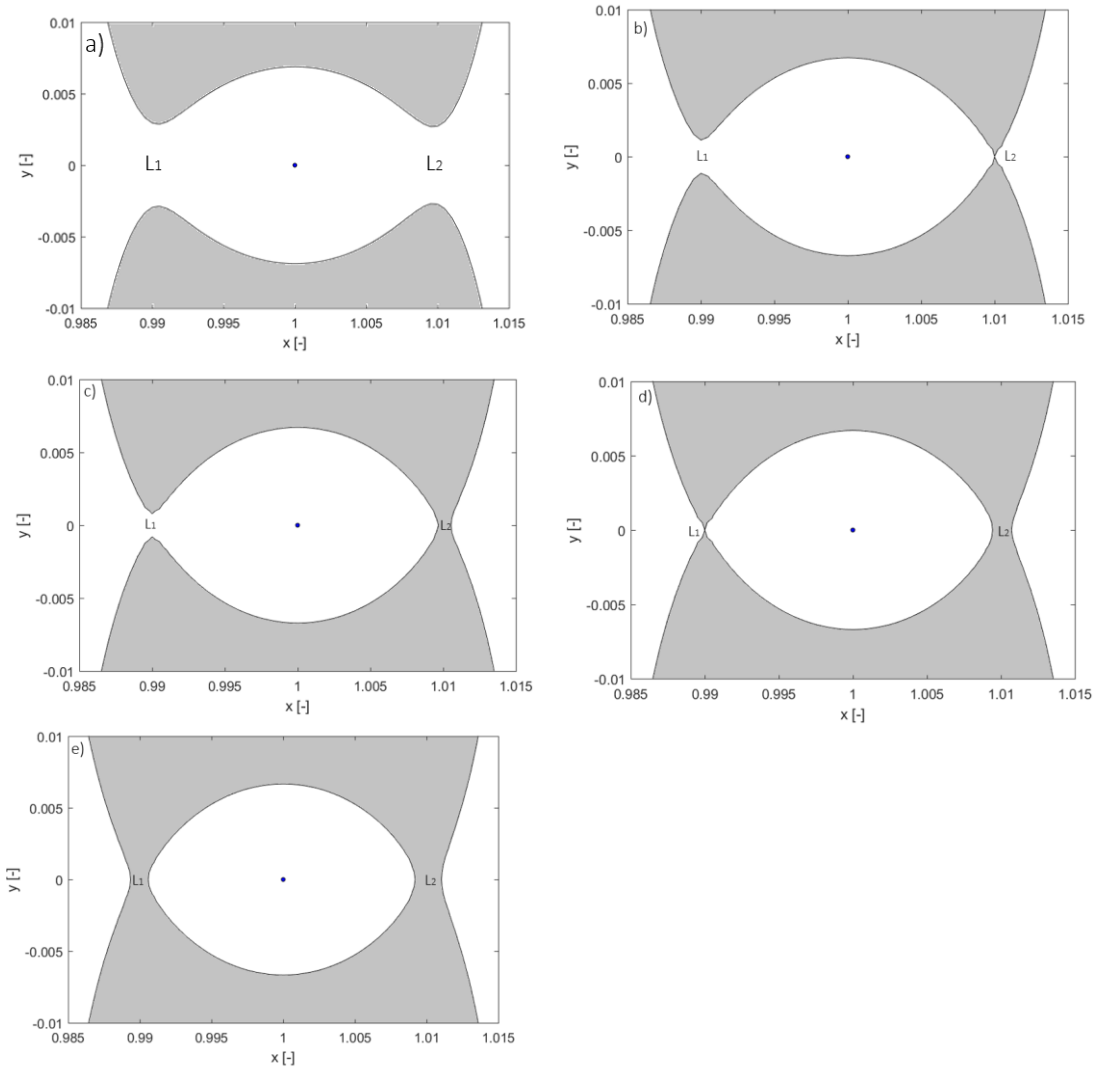

Fig. 6: Zero Velocity Curves representation for $J_{SC} = 2.9545$, $\vartheta_0 = 20°$ and different values of ϑ.

3.3 Two-impulse optimal disposal manoeuvre

The second method suggested to perform the heliocentric disposal is to give two manoeuvres and to optimise them selecting the best combination of the direction, α_1, β_1, and the magnitude Δv_1 for the first kick, and the time Δt_1 to wait to give the second one, which shall be less than 6 months, following [1]. To obtain the optimal disposal, a genetic algorithm was used. The algorithm was made of the following steps:

1. *Get the initial conditions*. In some case, it is required to start the disposal within a determined interval of time, thus, the initial ephemeris are taken within this range. Each state vector represents a different initial condition for the disposal, and it will be indicated with the subscript '0'. Thus, the initial state vector is named $\mathbf{s}_0$.
2. *First manoeuvre.* At the time instant $t = t_0$ the first burn is given. The variables Δv_1, α_1 and β_1 shall be optimised, and the components of the provided Δv are:

$$\begin{cases} \Delta v_{x1} = \Delta v_1 \cos\beta_1 \cos\alpha_1 \\ \Delta v_{y1} = \Delta v_1 \cos\beta_1 \sin\alpha_1 \\ \Delta v_{z1} = \Delta v_1 \sin\beta_1 \end{cases} \quad (18)$$

The term Δv_1 is dimensionless, and it is obtained by dividing the dimensional Δv by $r\dot{\vartheta}$, where r that is defined by Eq. (3)

, while $\dot{\vartheta}$ by Eq. (19).

$$\dot{\vartheta} = \frac{\left((\mu_1 + \mu_2)(1 + e\cos\vartheta)\right)^{\frac{1}{2}}}{\left(a(1 - e^2)\right)^{\frac{3}{2}}} \quad (19)$$

Moreover, if the efficiency is provided, this Δv_1 is rescaled in accordance with the efficiency, remembering that it depends on the orientation of the spacecraft [5].

The three Δv components showed in Eq. (18) are added to the velocity of the considered initial state vector $\mathbf{s}_0$, which then becomes:

$$\mathbf{s}_0 = \begin{cases} x_0 \\ y_0 \\ z_0 \\ v_{x0} + \Delta v_{x1} \\ v_{y0} + \Delta v_{y1} \\ v_{z0} + \Delta v_{z1} \end{cases} \quad (20)$$

3. *First leg*. The equations of motion defined in Eq. (7) are integrated for a time interval which goes from t_0, the day in which Δv_1 is given, up to $t_0 + \Delta t_1$. This interval is converted in the corresponding ϑ span, since the equation of motion are expressed in a pulsating reference frame. To integrate the equations of motions the MATLAB *ode113* solver, with an absolute and relative tolerances of 10^{-12}, has been used. The initial conditions were the ones defined in Eq. (20).
4. *Second manoeuvre.* The magnitude of the second manoeuvre shall be dimensionless. Thus, the dimensional

$$\Delta v_2 = \Delta v_{available} - \Delta v_1 \quad (21)$$

shall be divided by $r\dot{\vartheta}$, as already explained in point 2. If the magnitude of the Δv_2, is higher with respect to the one of the velocity of the spacecraft at the end of the propagation done in point 3, which is $v_{l_{end}}$, the Δv_2 shall be rescaled in the following way, in agreement with [4]:

$$\Delta v_2 = \min(\Delta v_{available} - \Delta v_1, v_{1_{end}}) \quad (22)$$

To reduce the energy of the spacecraft to close the ZVCs as much as possible, the Δv_2 shall be given in the opposite direction (in the rotating frame) with respect to the direction of the spacecraft velocity at time $t_0 + \Delta t_1$.

Then, calling $\alpha_{1_{end}}$ and $\beta_{1_{end}}$, respectively, the in-plane and the out-of-plane angle of $v_{l_{end}}$ with respect to the synodic reference frame, the direction of Δv_2 is determined by the angles $\alpha_2 = \alpha_{1_{end}} + \pi$ and $\beta_2 = -\beta_{1_{end}}$. Thus:

$$\Delta \mathbf{v}_2=[\Delta v_{x2}, \Delta v_{y2}, \Delta v_{z2}] \quad (23)$$

where the elements are equal to:

$$\Delta v_{x2} = \Delta v_2 \cos\beta_2 \cos\alpha_2 = -\Delta v_2 \cos\beta_{1_{end}} \cos\alpha_{1_{end}}$$

$$\Delta v_{y2} = \Delta v_2 \cos\beta_2 \sin\alpha_2 = -\Delta v_2 \cos\beta_{1_{end}} \sin\alpha_{1_{end}}$$

$$\Delta v_{z2} = \Delta v_2 \sin\beta_2 = -\Delta v_2 \sin\beta_{1_{end}}$$

Consequently, the initial state vector for the second propagation turns into:

$$\mathbf{s}_1 = \begin{cases} x_{1_{end}} \\ y_{1_{end}} \\ z_{1_{end}} \\ v_{x1_{end}} + \Delta v_{x2} \\ v_{y1_{end}} + \Delta v_{y2} \\ v_{z1_{end}} + \Delta v_{z2} \end{cases} \quad (24)$$

5. *Second leg*. The second propagation has been set to 100 years, to be sure that after 100 years from the disposal the spacecraft does not return in proximity of the Earth, as the planetary protection requirements imposes.
6. *Objective function*. The last passage of the optimisation is the evaluation of the objective function. In this paper, two objective functions were considered and used: the first is the one to obtain the *optimised disposal* which does not re-enter into the Earth's vicinity within 100 years of propagation, while the aim of the second one is to obtain a *sustainable disposal*, valid for more than 100 years of propagation, in compliance with the planetary protection requirements [20]. The chosen objective function is similar to the one used by Colombo et al. [5]. The used objective function which shall be minimised during the optimisation process, is defined as:

$$\text{Obj} = \log \frac{J_{LP,max@CA}}{J_{SC,2}} + P \quad (25)$$

The term $J_{SC,2}$ is the Jacobi constant of the spacecraft on the second leg, which is constant for any ϑ, red straight line in

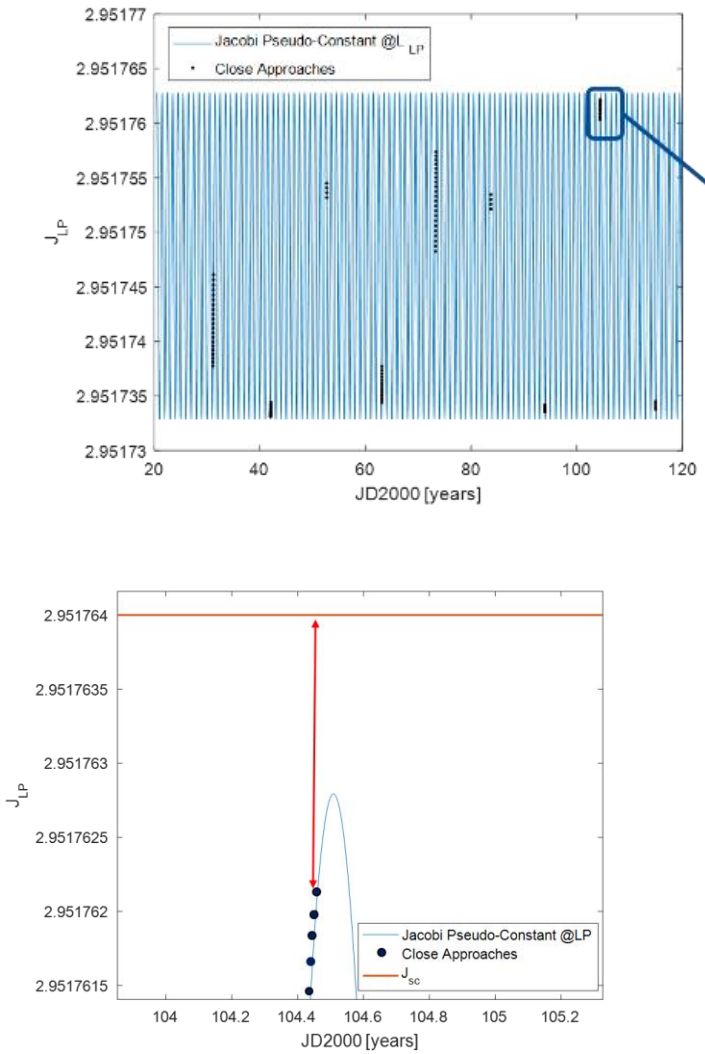

Fig. 7, on the bottom. On the top, the blue curve represents the evolution of the Jacobi pseudo-constant value for which the ZVCs are closed at the considered libration point, while the back dots represent the CAs. The term $J_{LP,max@CA}$ is defined as:

$$J_{LP,max@CA} = \max(ZVC_{LP}@CAs) \quad (26)$$

where the considered close approaches are only the one referred to the second leg. The minimisation of this function means the maximisation of the distance indicated by the red arrow in

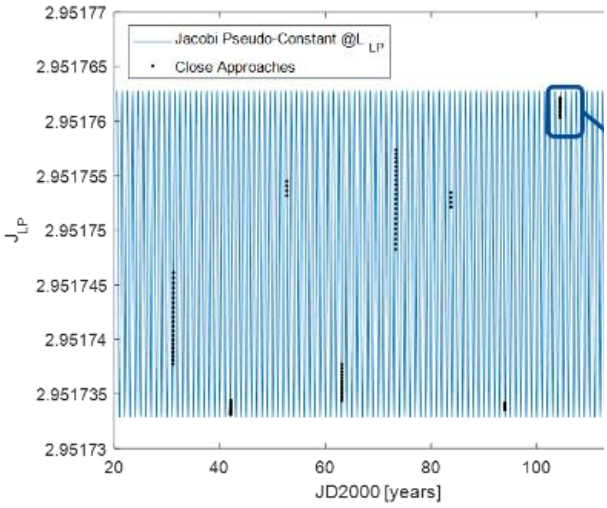

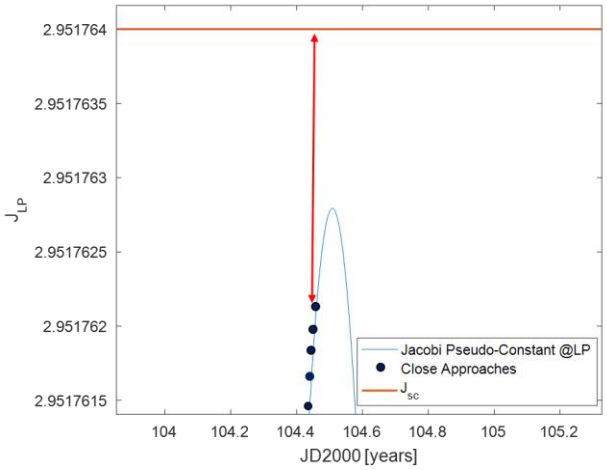

Fig. 7, which means that we attempt to close, as much as possible, the ZVCs.

The last term, $P = 10^{20}$, is a penalty factor that is assigned to the solutions that arrive too close to Earth (distance from Earth lower than $1.2 \cdot 10^6$ km, Colombo et al. [5]) or to the one which the resulting trajectory goes in the a wrong direction direction, such that it will approach the Earth.

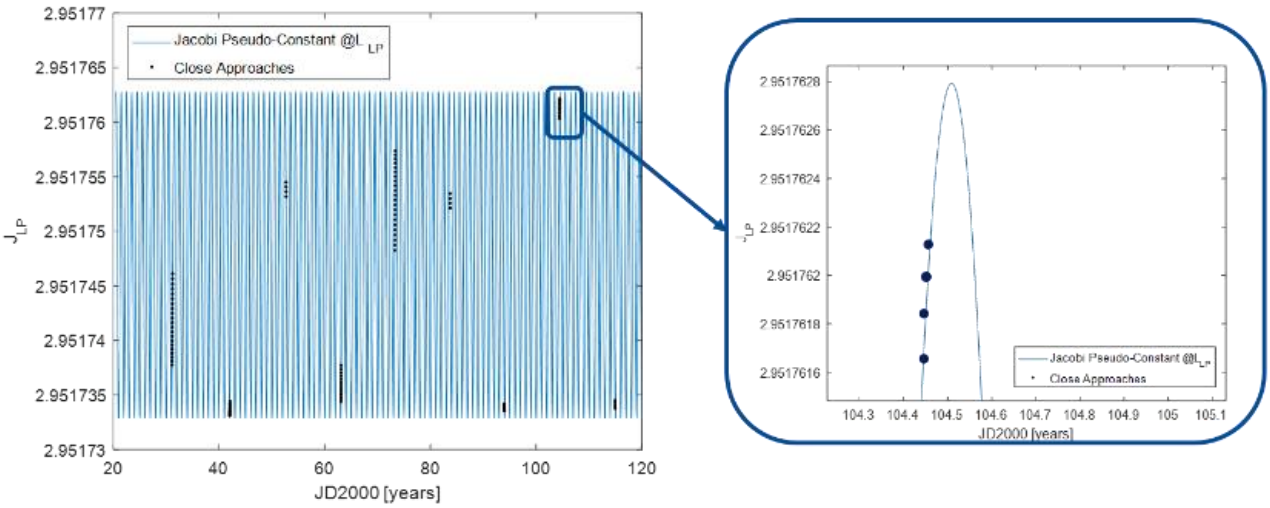

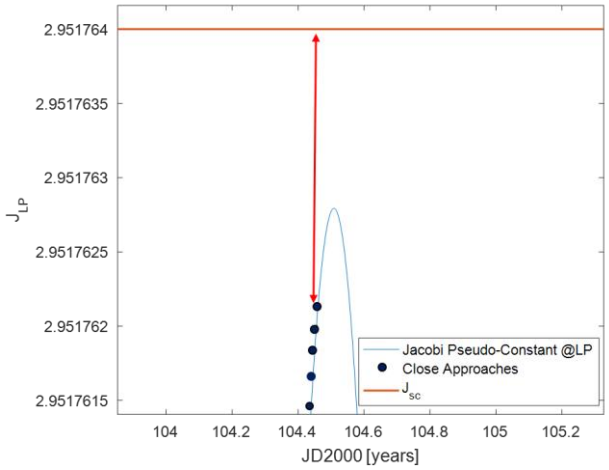

Fig. 7: Graphical representation of the objective function minimisation.

4 Results

4.1 Lisa Pathfinder

Lisa pathfinder had 6-months period Lissajous orbit around L_1 and an available Δv of 1 m/s. The departure dates were considered in the period going from 2016-10-30 to 2017-10-30, with a time span of 6 days. For each selected date, the optimisation was performed and the best combination of parameters as explained in Section 3 was found. The Fig. 8 shows the objective function, Eq. (25), value for each initial time, in red it is represented the single manoeuvre case while in blue the optimised two-burn manoeuvre. In both cases the objective function is positive, this means that the Jacobi pseudo-constant of the spacecraft value is always lower than the one evaluated at L_1, meaning that the propellant available is not enough to close the ZVCs. However, the Jacobi constant value is lower for the two-burns optimised strategy, which indicated that in this case the bottleneck at L_1 is smaller than the one in the single burn strategy. In conclusion, even if the Δv is low, if there is the possibility to perform a study to know which are the optimised disposal parameters for a two-burn disposal manoeuvre, it is better to proceed in this direction, to obtain the safer disposal possible. Indeed, a smaller gateway means lower probability for the spacecraft to cross the bottleneck and to come pack Earth in this way. In Fig. 8, it can be noticed that there are four local minima.

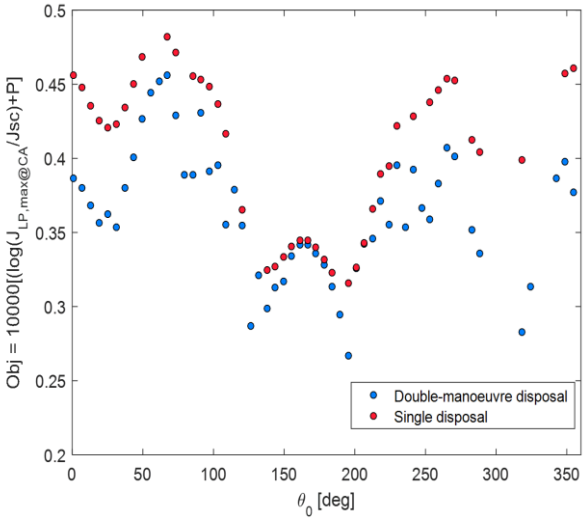

Fig. 8: Objective function value with respect to the true anomaly of the Earth in the moment in which the disposal started.

The studies performed showed that the two centre ones could be related with the maximum geometrical distance between Earth orbit and Lissajous, before the disposal. In other words, if the Δv is not enough to close the ZVCs, it is better to perform the disposal in a day in which the distance between the two orbit is maxima.

4.2 Gaia

Gaia spacecraft is orbiting on a six-months period Lissajous orbit around L_2 and the considered available Δv was the one given in [5], of the value of 275 m/s. The time span of initial condition went from 2019-01-01 to 2020-01-01. For every initial condition, Fig. 9 shows that the objective function is less than zero, meaning that the Δv is more than enough to close the gateway at L_2. On the other side, Fig. 10 indicates that the single manoeuvre strategy, even if the Δv is high, does never allow the closure of the ZVCs. Even in this case it appears that the strategy with two manoeuvre and the optimisation represent the best solution.

In this case, the optimal objective function has two local minima in correspondence of $\vartheta_0 = 0°$ and $\vartheta_0 = 180°$.

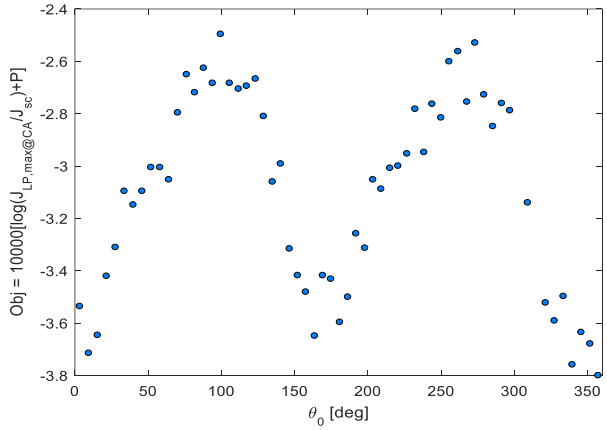

Fig. 9: Objective function value obtained optimising the two-burns disposal strategy.

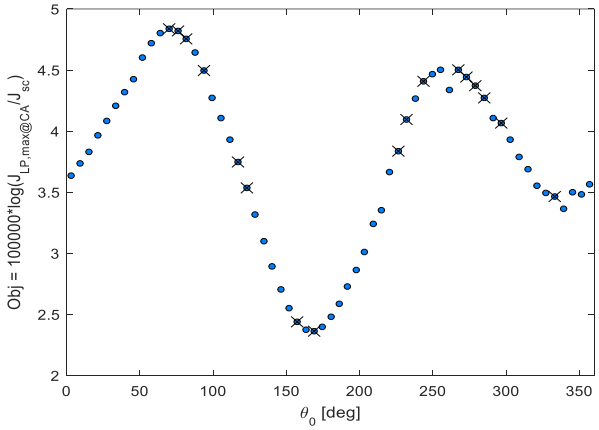

Fig. 10: Objective function value obtained with the single-burn disposal strategy. The solution indicated by the 'x' are the ones which come too close to Earth.

5 Analysis of Lisa Pathfinder return probability

Jehn and Renk in [21] analysed the Earth return probability for Lisa pathfinder using SNAPPshot [20], a tool for computing the planetary protection compliance. The simulation was done considering a Δv = 2 m/s, given within a time interval from 2016-10-30 to 2017-10-30 and the results are the one obtained in Fig. 11 where four local minimum can be easily individuate. The here is to understand, using the ER3BP model and the objective function defined in this paper in Section 3, This study leads to the conclusion that those could be related with the maximum difference between the Earth and Gaia phases at the departure. Moreover, the absolute minima was the same obtained using a more precise n-body model by Colombo et al. [5], which confirms that the ER3BP used here is a useful and simpler model to study the disposal from orbit around libration points. The simulations also showed that the direction of the first burn is given in the direction which leads the spacecraft to enter the unstable manifold. The fact that that Δt_1 resulted almost equal to six months, leads to the conclusion that the best manoeuvre is the one which aim to be a pseudo-Hohmann, in accordance with [5].

the reason behind the existence of the four local minima, shown in different colours in Fig. 11.

Our study leads to the conclusion that those could be related with the following quantities:

- The maximum geometrical distance between the two orbits (yellow minimum), as shown in Fig. 12 by the red curve. This means that, if there is only one disposal manoeuvre, it would be better to perform that when the spacecraft and the Earth are as far as possible one from each other.
- The maximum absolute relative phasing between Lisa Pathfinder and the Earth (red, purple and blue

minima), Fig. 13. Even in this case, the best solution is represented by the maximum angular distance between spacecraft and Earth.

- The angle between the Earth and the projection of Lisa Pathfinder pericentre orbit onto the ecliptic plane.

The Fig. 14 shows the objective function value (see Eq. (25)) for each initial condition in which the disposal is performed. Some minima and maxima are caught by our proposed objective function, while some other are not. The fact that some are caught could be seen as a further proof that the ER3BP and the objective function defined in this paper could be considered for a preliminary study on the disposal of spacecraft in libration points orbits. The minima and maxima that are not caught could be due to the fact that SNAPPshot uses a more precise model which, for example takes into account solar radiation pressure or the effect of all the bodies in the Solar system.

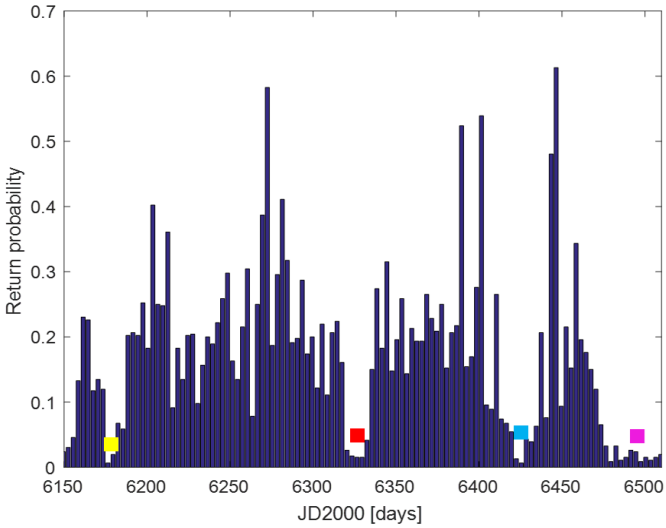

Fig. 11: Earth return probability for Lisa pathfinder.

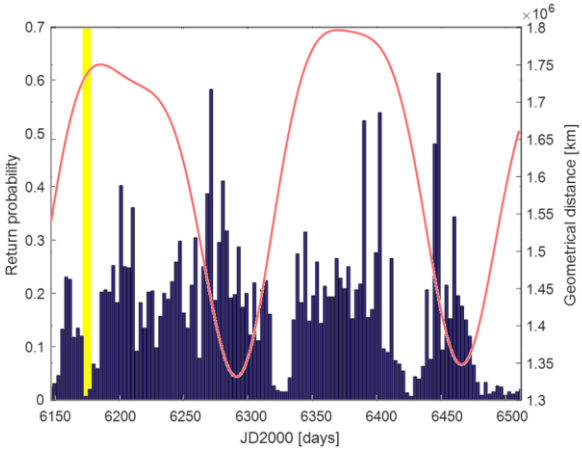

Fig. 12: Maximum geometrical distance between Earth and Lisa pathfinder orbits with respect to different initial condition over one year.

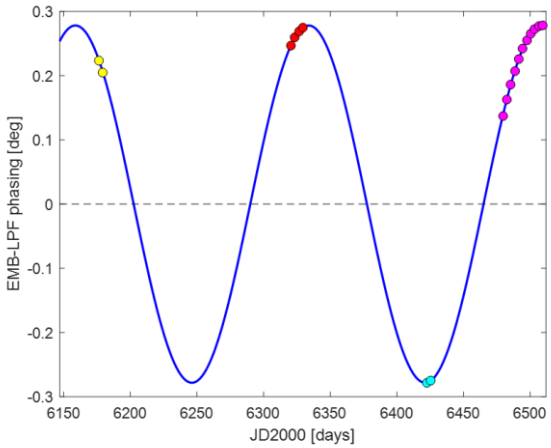

Fig. 13: Relative phasing Earth and Lissajous.

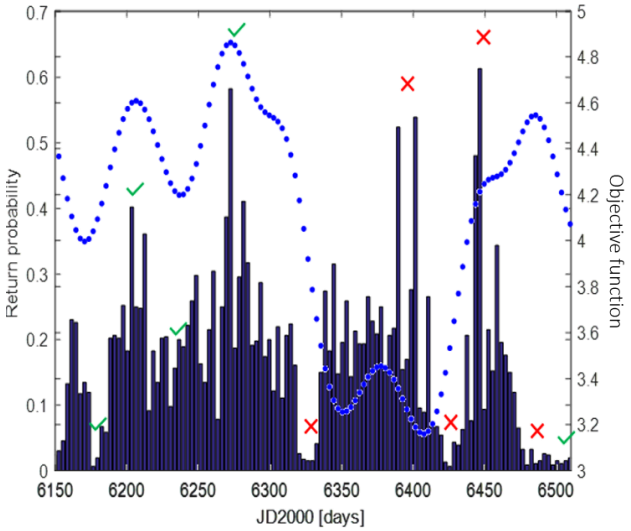

Fig. 14: LPF return probability compared with sustainable objective function obtained disposing LPF with one manoeuvre in Sun direction and using 2 m/s.

6 Conclusion

In this paper we used the ER3BP to design and to study the optimal disposal manoeuvre for spacecraft orbiting libration points. That was done through considering the pulsating behaviour of the zero velocity curves. Moreover, this paper tried to give an analytical and simple interpretation of the obtained results, added with an attempt to explain why there are some local minimum in the return probability analysis for Lisa pathfinder spacecraft.

In conclusion, the ER3BP could be a good model to study the disposal of spacecraft around the libration points. Moreover, if there are no constraint it should be better to optimise the disposal, together with the two-burn disposal solution, to decrease as much as possible the probability to return to Earth. Among the optimised solutions, the optimal ones are related with the true anomaly of Earth in correspondence of when the first disposal manoeuvre is given and with the initial geometrical distance between the Earth and the spacecraft orbits.

Regarding the Lisa Pathfinder return probability analysis, the minima could be related with the relative phasing between the Earth and the spacecraft, with the phasing between Earth and the projection onto the ecliptic of the Lisa pathfinder orbit pericentre, and with the maximum geometrical distance between the two initial orbits. In the future the used model can be improved considering also the effects of Moon and solar radiation pressure.

7 Acknowledgments

This work was supported by the European Research Council (ERC) under the European Union's Horizon 2020 research and innovation programme as part of project COMPASS (Control for Orbit Manoeuvring through Perturbations for Application to Space Systems), grant agreement 679086.

8 References

[1] Z. Olikara, G. Gòmez and J. Masdemont, "Dynamic Mechanism for Spacecraft Disposal from Sun-Earth Libration Points," *Juornal of guidance, control and dynamics,* vol. 38, no. 10, pp. 1976-1989, 2015.

[2] C. Colombo, F. Letizia, S. Soldini, M. Vetrisano, M. Vasile, A. Rossi, M. Landgraf, W. Van der Weng, "End-of-life disposal concepts for libration point andhighly elliptical orbit missions," 2014.

[3] E. Alessi, «The Reentry to Earth as a Valuable Option at the End-of-Life of Libration Point Orbit Missions,» *Advances Space Research,* vol. 55, n. 12, pp. 2914-2930, 2015.

[4] C. Colombo, F. Letizia, S. Soldini, E.M. Alessi, M. Vasile, M. Vetrisano and W. van der Weng, "End-Of-Life Disposal Concepts for Lagrange-Point and Highly Elliptical Orbit Missions, Final Report, Gaia and LISA Pathfinder heliocentric disposal, Gaia re-entry," ESA/ESOC contract No. 4000107624/13/F/MOS, 2014.

[5] C. Colombo, F. Letizia, S. Soldini e F. Renk, "Disposal of libration point orbits on a heliocentric graveyard orbit: the Gaia mission", *Advances in Space Research,* vol. 56, 2015.

[6] S. Soldini, C. Colombo and S. Walker, "Solar radiation pressure enhanced disposal in the Elliptic Restriceted Three Body Problem: application to the Gaia mission," *Advances in Space Research,* vol. 57, pp. 1664-1679, 2016.

[7] F. Z. Luo e F. Topputo, "Analysis of ballistic capture in Sun-planets models", *Advances in Space Research,* vol. 56, n. 6, pp. 1030-1041, 2015.

[8] N. Hyeraci e F. Topputo, "A Method to Design Ballistic Capture in the Elliptic Restricted Three-Body Problem", *Journal of Guidance, Control and Dynamics,* vol. 33, n. 6, pp. 1814-1823.

[9] S. Solidini, *Design and Control of Solar Radiation Pressure Assisted Missions in the Sun-Earth Restricted Three-Body Problem,* PhD thesis University of Southampton, Supervisors S. Walker, C. Colombo, Southampton , 2016.

[10] W. Koon, W. Lo, J. Marsden and S. Ross, Dynamical Systems, the Three-Body Problem, 2005.

[11] G. Gomez, J. Llibre, R. Martinez and C. Simò, Dynamic and Mission Design Near Libration Points, Vol. I Fundamentals: The case of Collinear Libration Points, 2000.

[12] G. Colasurdo e G. Avanzini, Astrodynamics, Torino: SEEDS, SpacE Exploration and Development Systems, 2006.

[13] L. G. Luk'yanov, "Energy Conservation in the Restricted Elliptical Three-Body Problem," *Astronomy reports,* vol. 49, no. 12, p. 1018–1027 , 2005.

[14] V. Szebehely and E. Grebenikov, "Theory of orbits in the restricted problem of three bodies," *Soviet Astronomy,* vol. 13, pp. 364-366, 1967.

[15] S. Campagnola, L. Martin e P. Newton, «Subregions of motion and elliptic halo orbits in the elliptic restricted three-body problem.,» 2008.

[16] M. Rasotto, P. Di Lizia, F. Renk, R. Armellin, "End-of-life disposal for libration point orbit missions: The case of Gaia," *Advances in Space Research,* vol. 56, n. 3, pp. 416-478.

[17] C. Colombo, F. Letizia, S. Soldini, M. Alessi, M. Vasile, M. Vetrisano and W. van der Weg, "End-Of-Life Disposal Concepts for Lagrange-Point and Highly Elliptical Orbit Missions - Final Report Gaia and LISA Pathfinder heliocentric disposal, Gaia re-entry," ESA/ESOC contract No. 4000107624/13/F/MOS, 2014.

[18] S. D. Ross, Cylindrical Manifolds and Tube Dynamics in the Restricted Three-Body Problem, Pasadena, California: Dissertation (Ph.D.), California Institute of Technology, 2004.

[19] G. De Marco, «Appendix A3,» in *End-of-life Disposal Design for Spacecraft at Libration Points Orbits and an Interpretation of Their Probability of Earth Return*, Politecnico di Milano, Faculty of Industrial Engineering, Department of Aerospace Science and Technologies, Master in Space Engineering, Advisor: Camilla Colombo, 2018.

[20] F. Letizia, C. Colombo, J. Van den Eynde, R. Armellin e R. Jehn, «SNAPPSHOT: Suite For The Numerical Analysis for Planetary Protection,» in *6th International Conference on Astrodynamics Tools and Techniques*, 2016.

[21] R. Jehn e F. Renk, «Impact Of Space Debris Mitigation Requirements On The Mission Design Of ESA Spacecraft,» in *Proc. 7th European Conference on Space Debris*, Darmstadt, Germany, 18 - 21 April 2017.